Available online at www.sciencedirect.com

ScienceDirect

Procedia Engineering 120 (2015) 341 – 344

Procedia Engineering

www.elsevier.com/locate/procedia

EUROSENSORS 2015

Electret-based Out-Of-Plane Micro Energy Harvester with Parylene-C Serving as the Electret and Spring Material

S. Genter*, T. Langhof and O. Paul

Department of Microsystems Engineering (IMTEK), University of Freiburg, Germany

Abstract

A micro energy harvesting device based on electrostatic transduction using Parylene-C as the electret layer and spring material of an out-of-plane generator (OoPG) is presented. This approach is advantageous for three reasons. First the fabrication of the device can be realized with simpler processing steps compared to in-plane configurations. Second, being unstructured the electret has a larger area and can be charged more effectively by a corona discharge. As a consequence, thirdly, the output power is potentially higher. In this paper the design, fabrication and characterization of such an OoPG are described.

Peer-review under responsibility of the organizing committee of EUROSENSORS 2015

Keywords: Enery Harvesting, Electret, Out-of-Plane, Corona Discharge, Parylene-C

1. Introduction

Various electret-based micro energy harvesters have recently been proposed [1-3]. In a common approach, they rely on an in-plane moving electrode with a comb-shaped electret layer helping to reduce the necessary oscillation amplitudes and to increase the expected output power. However structured, narrow electret lines suffer from edge effects when being charged and offer a smaller effective area. In contrast OoPGs can be fabricated with an unstructured electret layer [4,5]. Thus, the area of the electret layer can be maximized and furthermore the charging process can be performed more effectively. In this work, this geometry is combined with a simple fabrication process using the polymer Parylene-C for the suspension of the moving electrode and as the electret layer to build an OoPG. We thus exploit the mechanical and electret properties of this material.

* Corresponding author: Simon Genter. Tel.: +49-761-203-7193; fax: +49-761-203-7912.
E-mail address: simon.genter@imtek.uni-freiburg.de

Peer-review under responsibility of the organizing committee of EUROSENSORS 2015
doi:10.1016/j.proeng.2015.08.630

2. Design and Fabrication

The device consists of a base chip and a resonator chip both made of highly conducting 4-inch-silicon wafers, as shown in Fig. 1. Two inductively coupled plasma (ICP) etching steps realize indentations in the base chip defining a 25-µm-deep alignment structure for the resonator chip and the gap between the two electrodes with a depth of 50 µm (Fig. 1(a)). The top surface of the wafer is covered by an evaporated Cr/Au metallization and a structured SiOx/SiN passivation deposited by plasma enhanced chemical vapor deposition (Fig. 1(b)).

The resonator chip is also covered by a Cr/Au stack, topped by a 7.5 µm Parylene-C layer (Fig. 1(c)). The Parylene-C layer is structured using reactive ion etching (RIE) with an oxygen plasma to define bonding pads. The circular seismic mass with an area A_{res} = 4-36 mm² is released by rear ICP etching (Fig. 1(d)) which stops Cr layer of the resonator metallization. A second 7.5-µm-thick Parylene-C layer deposited on the rear serves as the functional electret layer and as electrical isolation (Fig.1 (e)). In summary, the flexural suspension is $d_{ring} \approx 15$ µm thick and w_{ring} = 0.5-1.5 mm wide.

For the assembly of the resonator and base chips, the corona-charged resonator chip is placed into the indentations of the base-chip and fixed using a two-component epoxy (Fig.1 (f)). This assembly is performed at room temperature (RT) to prevent a thermally induced discharge of the charged electret layer. A fabricated device is shown in Fig. 2.

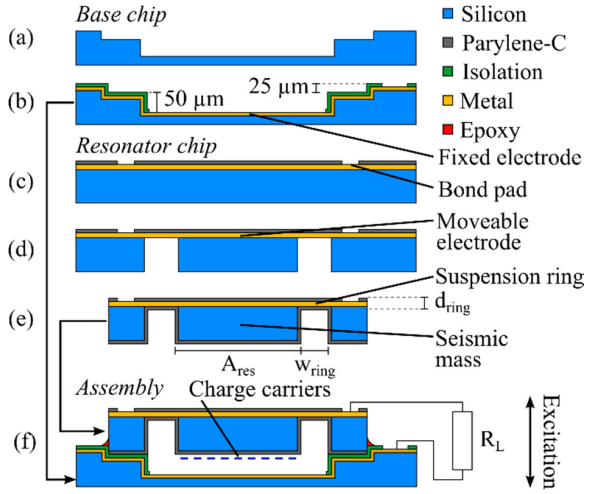

Figure 1: Schematic views of the fabrication of the base and resonator chips and of their assembly.

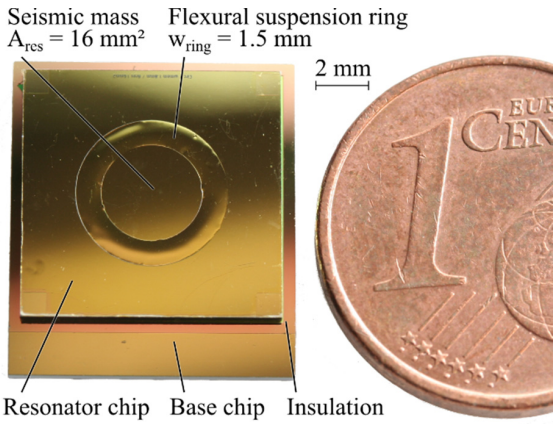

Figure 2: Photograph of a fabricated micro-generator with w_{ring} = 1.5 mm, A_{res} = 16 mm² and d_{ring} = 15 µm in comparison with 1-€-Cent coin.

3. Experimental

3.1. Mechanical Response

First, the mechanical response of the resonators was investigated using the TiraVib BAA-120 shaker from *TIRA* and the MSA-400 dynamic microsystem analyzer from *Polytec* serving for the mechanical excitation of the microstructures and for measuring their frequency-dependent out-of-plane amplitudes, respectively. The results for an exemplary device with an electret area of A_{res} = 4 mm² and a suspension width of w_{ring} = 1 mm are shown in Fig. 3. The excitation voltage V_{Gen} was applied to the amplifier of the shaker. It was varied between 2 V and 6 V in 2 V steps where 1 V corresponds to an acceleration of 1 g. With this configuration, maximum amplitudes of about 10 µm, 20 µm and 25 µm at resonant frequencies f_{res} of 3 kHz 3.055 kHz and 3.175 kHz where measured, respectively. Besides the increasing resonant frequency, the bandwidth also increases due to spring hardening. The increasing non-linearity of

the mechanical response at higher amplitudes is also indicated by the increasing hysteresis between the corresponding upward and downward sweeps.

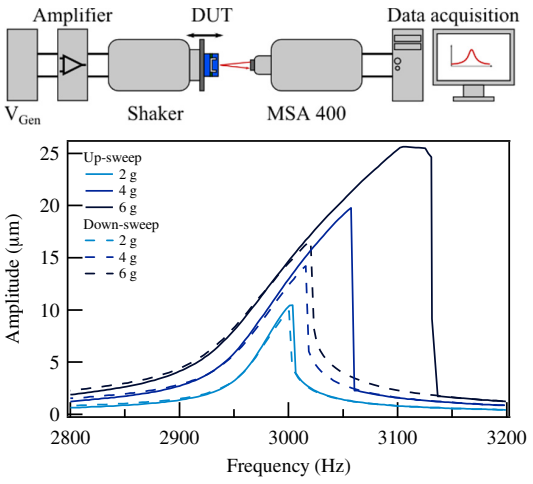

Figure 3: Measured mechanical amplitudes of a resonant mass with A_{res} = 4 mm² and w_{ring} = 1 mm for three excitation accelerations.

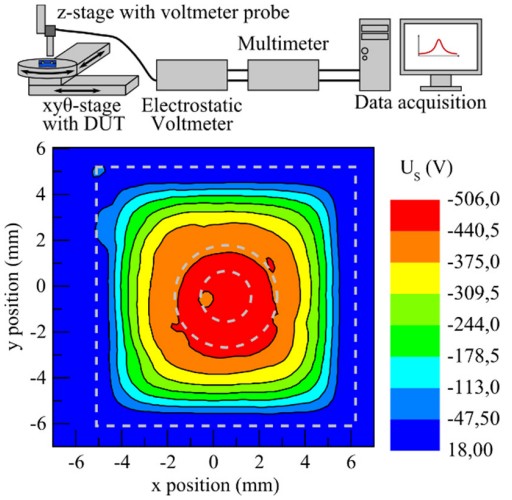

Figure 4: Measured surface potential U_S of the electret layer on the resonator chip. The dashed lines indicate the geometry of the resonator chip.

3.2. Electret Charging

Furthermore, the electrical characterization of the device is performed. For this purpose, the electret layer on the resonator is charged at RT for 3 min using a custom-made corona discharge setup [6,7]. Charge carriers are generated at a sharp needle tip with the potential of −8 kV. Between the needle tip and the device at ground potential a second, mesh-shaped electrode is set to a potential of −800 V to control the resulting surface potential U_S of the electret layer. As shown in Fig. 4, U_S values exceeding −500 V are achieved in the area of the movable seismic mass outlined by the central circle among the gray dashed lines corresponding to the geometry of the device under test.

3.3. Electrical Response

For the electrical output power values P_{out} reported in Figs. 5 and 6, a device with A_{ring} = 4 mm² and w_{ring} = 1 mm was excited at f_{res} = 3 kHz. In Figure 5, the load resistor R_L is varied between 0.5 MΩ and 5 MΩ. For increasing values of R_L, the generated output first increases before reaching a maximum point at the optimal value of 1.24 MΩ for this configuration. This optimal load is valid for all three excitations with a resulting output power of 0.07 nW, 0.34 nW and 0.7 nW, respectively. The further increase of R_L leads to a decreasing output power. The variation of V_{Gen} in Fig. 6 is performed at the optimal R_L value of 1.24 MΩ. Increasing V_{Gen} from 0 V to 10 V generates P_{out} values with a quadratic dependence on V_{Gen}.

Other samples with different geometries were also investigated. Using a larger area A_{ring} should result in higher P_{out} values, theoretically. However, due to the larger area, the electrostatic forces are also increasing and a pull-in of the moving electrode with the highly charged electret layer to counter-electrode occurred. As a consequence it was no longer possible to excite the device and to extract any power from it. To avoid the pull-in effect, a mechanical stop-mechanism using studs or bumpers should be implemented or the gap size and spring stiffness could be adjusted.

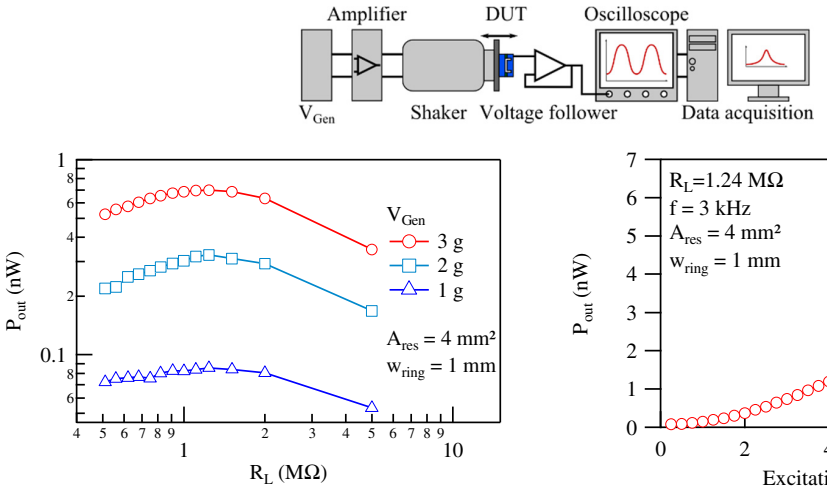

Figure 5: Measured output power P_{out} as a function of the load resistor R_L using different excitation accelerations.

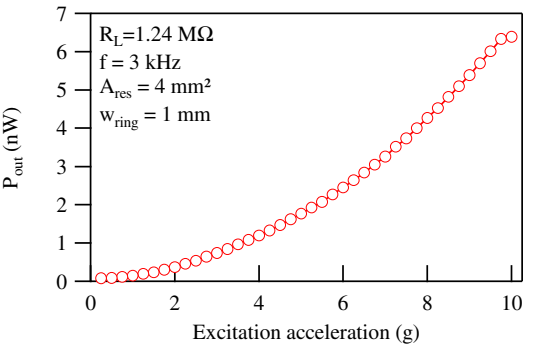

Figure 6: Measured output power P_{out} as a function of the excitation acceleration.

4. Conclusion

A particular appeal of the present solution stems from the fact that Parylene-C serves as a multi-functional material with electrical and mechanical functions. Thereby the complexity of the device fabrication was reduced. Using geometries of A_{res} = 4 mm² and w_{ring} = 1 mm, an optimal load of 1.24 MΩ was determined to result in generated output power values up to several nW. However, the design should be improved by including a mechanism preventing the pull-in effect of the movable electrode with the charged electret layer to the counter-electrode to guarantee the functionality of the device for a wider variety of design parameters. Furthermore, the design definitely leaves room for improvement regarding f_{res}, P_{out} and bandwidth. Higher P_{out} values at lower frequencies f_{res} with a large bandwidth are desirable.

References

[1] J. Boland et al., Micro Electret Power Generator, Proc. IEEE Int. Conf. MEMS, Kyoto (2003) 538-541
[2] M. Edamoto et al., Electret-Based Energy Harvesting Device with Parylene Flexible Springs, The 4th Asia Pacific Conference on Transducers and Micro/Nano Technologies (APCOT) (2008)
[3] K. Tao et al., A Sandwiched-Structured MEMS Electret Power Generator for Multi-Directional Vibration Energy Harvesting, Dig. Tech. Papers Transducers, Anchorage (2015), 51-54
[4] T. Takahashi et al., A Miniature Harvester of Vertical Vibratory Capacitive Type Achieving Several Tens Microwatt for Broad Frequency of 20-40 Hz, Dig. Tech. Papers Transducers, Barcelona (2012) 1340-1343
[5] F. Wang, O. Hansen, Electrostatic Energy Harvesting Device with Out-of-plane Gap closing scheme, Dig. Tech. Papers Transducers, Barcelona (2013) 2237-2240.
[6] U. Bartsch, J. Gaspar, O. Paul, Characterization of the Charging and Long-Term Performance of Cytop Electret Layers for MEMS Applications, Mater. Res. Soc. Symp. Proc. Vol. 1134, (2009) 1134-BB08-17
[7] S. Genter, O. Paul, Influence of Various Conducting and Inorganic Dielectric Drift Barriers on the Charge Decay in Parylene-C Electret Layers, Int. Conf. PowerMEMS 2014, Journal of Physics: Conference Series 557 (2014) 012102